JOURNAL OF MATERIALS SCIENCE 29 (1994) 4708–4712

Ageing effects during isothermal crystallization of polypropylene blended with elastomers

W. WENIG
University of Duisburg, Laboratory of Applied Physics, 47048 Duisburg, Germany

The secondary crystallization of isotactic polypropylene in its blend with the elastomers ethylene–propylene–diene–terpolymer (EPDM) and trans-polyoctenylene (TOR), which occurs during isothermal crystallization, has been measured by time-dependent recording of X-ray wide-angle scattering. From the results, Avrami exponents were determined, which show that secondary crystallization takes place primarily within the already formed spherulites. Avrami exponents of the primary crystallization have been determined by the same method and also by observation of the spherulitic growth in the polarization microscope. It was found that both elastomers have different effects on the crystallization behaviour of the polypropylene.

1. Introduction

The blending of elastomers to isotactic polypropylene (iPP) influences its mechanical behaviour [1]: while the impact strength of such blends is increasing, the elastic modulus is decreasing. It has been found that the course of the elastic modulus as a function of elastomer mass fraction in the blend is correlated with the statistical order of the lamellar morphology, and that the degree of dispersion of elastomer in the iPP matrix is the reason for the morphological changes [2]. This dispersion has an effect on the crystallization behaviour of the iPP matrix by influencing the interphase volume between the two components.

For blends of iPP with ethylene–propylene–diene–terpolymer (EPDM), Martuscelli *et al.* [3] found a strong dependence of crystallization parameters such as nucleation density and spherulite growth rate on the amount of EPDM mixed into iPP. When the EPDM is replaced by trans-polyoctenylene (TOR), the nucleation becomes more heterogeneous for certain TOR concentrations than for others, which has been shown to be a consequence of concentration-dependent dispersion of the rubber component in the iPP matrix [4].

A measure for the mode of nucleation is the Avrami exponent, which, for equal crystallization conditions, describes the transition from homogeneous to heterogeneous nucleation. Several methods for both isothermal and non-isothermal determination have been proposed [5–12]. Because for polypropylene the spherulite growth can be well monitored under the optical microscope, microscopic methods for isothermal determination of the Avrami exponent are often used. This method can only be properly used, when effects like secondary crystallization can be excluded. However, in the case of isothermal crystallization, this cannot always be assured. In neat polypropylene, a mixture of homogeneous and heterogeneous nucleation and secondary nucleation as an effect of ageing during isothermal crystallization seems to occur in most cases. Mixtures of iPP and elastomer show an even more complicated behaviour. Therefore, it would be of interest to separate primary and secondary nucleation. This is possible through direct measurement of the volume of the crystalline material transferred from the melt, i.e. the crystallinity of the sample, during crystallization by X-ray methods. These experiments are described here for the systems iPP/EPDM and iPP/TOR.

2. Experimental procedure

2.1. Sample preparation

Isotactic polypropylene ($M_W = 468\,000$), polyoctenylene ($M_W = 89\,000$, trans-content 80%) and ethylene–propylene–diene–terpolymer ($M_W = 215\,000$), were dissolved in hot *o*-xylene and precipitated into a large excess of methanol to form iPP/TOR and iPP/EPDM blends with elastomer contents of 0%, 5%, 10%, 15% and 20%, respectively. For each sample, a quantity of the dried material was placed between the plates of a hydraulic press and heated to a temperature well above the melting point under a force of 100 kN. After switching off the press, the sample was allowed to cool to room temperature. The resulting thickness of the samples amounted to $\sim 30\,\mu m$ for the microscopic investigations and ~ 1 mm for the X-ray experiments.

2.2. Measurements

For observation in the optical microscope (Leitz Metallux II) the samples were placed between microscope slides and placed in a Mettler hot stage, where they were heated to 200 °C for 5 min and then cooled to the chosen crystallization temperature, T_c. Crossed polarizers were used and the crystallization was monitored on a video screen, digitized, and recorded on a computer hard disk. The crystallization temperatures for the isothermal crystallization were chosen

0022–2461

between 130 and 140 °C. Each crystallization experiment was carried out five times at different locations on the sample for an error analysis.

X-ray wide-angle scattering curves were recorded using a Philips PW 1380 goniometer. The measurements were controlled by a computer, and the temperature of the cooling water was kept constant through a constant temperature unit. CuK_α radiation was used and monochromatization was achieved by use of a nickel filter in conjunction with pulse-height analysis. The goniometer was equipped with a Paar TTK-HC temperature chamber to investigate the samples at the chosen crystallization temperature. To monitor the development of crystallinity as a function of time, the scattering curves were measured in the angular range $7° \leqslant 2\theta \leqslant 30°$ with a stepsize of 0.125° and a counting time of 20 s. After subtracting the background, a separate measured halo was fitted to the curve [13–16].

3. Results and discussion

From X-ray measurements, the Avrami exponent can be determined through the well-known equation [17–20]

$$X_c(t) = 1 - \exp(-kt^n) \quad (1)$$

which describes the development of the crystallinity in a crystallizing spherulite as a function of time. X_c is the volume crystallinity as a function of crystallization time, t, k a characteristic constant, and n the Avrami-exponent describing the mode of crystallization. Plotting $\ln[-\ln(1 - X_c)]$ versus $\ln t$, the Avrami exponent is yielded from the slope of the straight line. Fig. 1 shows such plots for two examples: iPP mixed with 15% TOR (Fig. 1a) and with 15% EPDM (Fig. 1b) for all crystallization temperatures. The figures reveal two straight lines for every crystallization temperature with different slopes. The steeper lines yield the Avrami exponents for the primary crystallization, the second line with lower slope the secondary crystallization. We see that fewer points are obtained for the primary crystallization. The reason is that X-ray determination of the crystallinity does not limit the measurement of slow crystallization processes, but has limited sensitivity for fast processes (e.g. the error for X_c measured at $T_c = 130$ °C and $t_c = 25$ s crystallization time amounts to $\sim 5\%$, while for $t_c = 100$ min it decreases to $\sim 0.5\%$). Therefore, the values for n determined for low crystallization temperatures and short crystallization times have a lower accuracy. As repeated measurements showed, an error above 1% is found only for very short crystallization times and is independent of the elastomer content. The secondary crystallization, however, can be well monitored. The results are displayed in Fig. 2, where the Avrami exponents for both elastomers and for the two crystallization processes are shown. In Fig. 2a the values for the primary crystallization are plotted. For

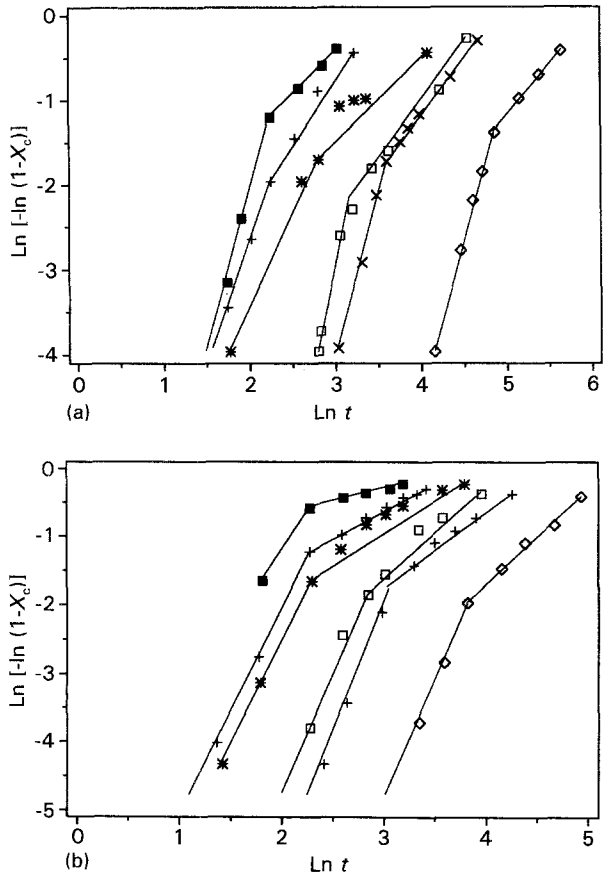

Figure 1 Avrami plot for iPP blended with (a) trans-polyoctenylene (85% iPP + 15% TOR) and (b) ethylene–propylene–diene–terpolymer (85% iPP + 15% EPDM) at different crystallization times: (■) 130 °C, (+) 132 °C, (★) 134 °C, (□) 136 °C, (×) 138 °C, (◇) 140 °C.

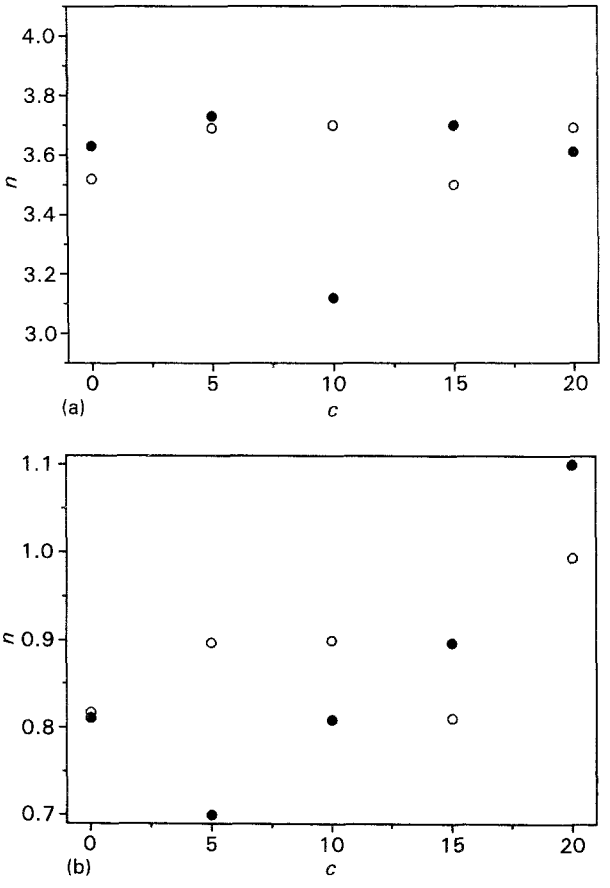

Figure 2 Avrami exponents for (a) primary and (b) secondary crystallization as a function of elastomer concentration. (●) TOR, (○) EPDM.

the given crystallization conditions, n should assume the values $n = 3$ for heterogeneous and $n = 4$ for homogeneous nucleation [20]. It can be seen from Fig. 2a, that for neat polypropylene n assumes a value lower than 4. This may be an effect of catalyst residues, but it seems that "natural" impurities are responsible for this behaviour [21, 22]. In unseeded PP, therefore, a mixture of heterogeneous and homogeneous nucleation is observed.

The addition of TOR or EPDM to iPP shows different courses for n for both elastomers: while for EPDM n varies only slightly with the concentration, the blend iPP/TOR shows a minimum for n at 10% TOR content ($n \sim 3$). Here the nucleation is almost entirely heterogeneous, which has been discussed earlier to be a consequence of an increasing iPP/TOR interphase due to a higher dispersion of the TOR component at this composition [2, 4]. The Avrami exponent of the iPP/EPDM blend does not show this dependence. Here, n varies only slightly with the EPDM content, showing only a small drop of n at 15% EPDM.

The Avrami exponent of the primary crystallization can also be determined from the observation of the spherulitic growth in the optical microscope.

Provided that the spherulites are globular shaped, and that their crystallinity is independent of their volume, the spherulitic volume, $V_{sph}(t)$, is proportional to the "absolute" volume, $V_{sph,abs}$, (the transferred volume covered by the crystals in the spherulites), and the observed volume, and thus proportional to the crystallinity, $X_c(t)$

$$V_{sph}(t) = \frac{V_{sph,abs}}{V_{obs}} \tag{2}$$

From the microscope image, only spherulitic areas instead of volumes can be determined. From the volume of the spherulitic globules, $V = 4/3\,\pi r^3$, the "half-radius", which is correlated to the half-volume, $V_{1/2}$, may be calculated

$$r = \left(\frac{3V}{4\pi}\right)^{1/3} \tag{3}$$

$$r_{1/2} = \left(\frac{3V_{1/2}}{4\pi}\right)^{1/3}\left(\frac{3V}{8\pi}\right)^{1/3} \tag{4}$$

The ratio of radius to half-radius corresponds to the ratio, $A_{1/2}$, of the respective areas covered by the spherulites. This ratio calculates

$$\begin{aligned} A_{1/2} &= \frac{r_{1/2}\pi}{r\pi} \\ &= \left[\frac{(3V)/(8\pi)}{(3V)/(4\pi)}\right]^{2/3} \\ &= \left(\frac{1}{2}\right)^{2/3} \\ &= 0.63 \end{aligned} \tag{5}$$

Thus, the spherulites cover half the volume, when 63% of the observed area is covered. From this the volume half time, $t_{v,1/2}$, can be determined.

For globular spherulites for athermal nucleation, $n = 3$ and

$$k = (4\pi/3)G_m^3 M \tag{6}$$

where G_m is the average spherulitic growth rate, and for thermal nucleation $n = 4$ and

$$k = (\pi/3)G_m^3 M(t) \tag{7}$$

where $M(t)$ describes the development of nuclei per unit volume as a function of time. For the shape of the spherulites discussed here, the term kt^n becomes the N-fold spherical volume

$$kt^n \approx (4/3)\pi G_m^3 M t^3 \tag{8}$$

We then obtain for the Avrami equation

$$V_{sph}(t) = 1 - \exp\left[-(4/3)\pi G_m^3 M t^n\right] \tag{9}$$

From this equation we calculate for n

$$-(4/3)\pi G_m^3 M t^n = \ln\left[1 - V_{sph}(t)\right] \tag{10}$$

$$t^n = \frac{3\ln\left[1 - V_{sph}(t)\right]}{4\pi G_m^3 M} \tag{11}$$

$$n = \log\left\{-\frac{3\ln[1 - V_{sph}(t)]}{4\pi G_m^3 M}\right\} \Big/ \log t \tag{12}$$

With $t = t_{v,1/2}$, Equation 12 becomes

$$n = \log\left[-\frac{3\ln 2}{4\pi G_m^3 M}\right] \Big/ \log t \tag{13}$$

The Avrami exponent can thus be determined by measuring the spherulitic growth rate, the nucleation density, and the volume half-time.

The values for n determined by this method are displayed in Fig. 3. We see that we obtain n varying around 3.5 and the same principal concentration dependence. These results show, that the determination of the Avrami exponent by observation of the spherulitic growth can obviously be done with sufficient accuracy, despite the fact that the sample is squeezed into a limited volume between the microscope slides [23].

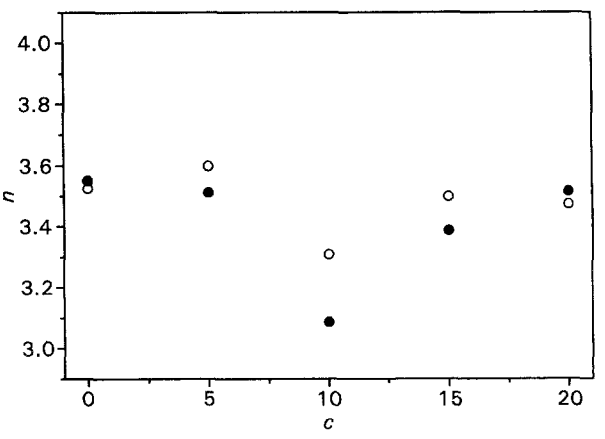

Figure 3 Avrami exponents of the primary crystallization, determined by microscopic observation of the spherulitic growth, as a function of elastomer concentration. (●) TOR, (○) EPDM.

The sharp drop of n at 10% TOR in the iPP/TOR blend should be accompanied by a change of the spherulitic radius and its distribution. For this blend, one can observe in the microscope, that the spherulitic size distribution is small at 10% TOR and significantly higher for all other concentrations.

The mean spherulitic radius can be determined from the micrographs as follows: having determined the nucleation density, M, the mean spherulitic volume can be calculated as

$$\bar{V}_{\text{sph}} = \frac{1}{M} = (4/3)\pi(\bar{r})^3 \quad (14)$$

From this equation the mean spherulitic radius can be determined

$$\bar{r} = \left(\frac{3}{4\pi}\frac{1}{M}\right)^{1/3} \quad (15)$$

From Fig. 4, where $\bar{r}$ as a function of the TOR concentration is shown, the mean spherulitic radius is seen to surpass a minimum at 10% TOR.

Owing to its longer crystallization time, the secondary crystallization, which is discussed in the literature as an ageing process [9, 11], can be well monitored by X-ray measurements. Several concepts have been developed concerning the location of secondary crystallization and the orientation of the crystals. It is known that ageing leads to an improved tensile strength, which is believed to be a result of decreasing spherulite size [24, 25]. Vinogradskaya *et al.* [26] proposed the crystallization of small spherulites in the interspherulitic zones between the spherulites of primary crystallization, but other microstructural variations could also be possible. Gezovich and Geil [27] suggested an orientation in the amorphous zones, and Remaly and Schultz [11] assumed additional structural rearrangements after the formation of the spherulitic microstructure. Interspherulitic crystallization could explain the measured increase of crystallinity at longer crystallization times. Whether the secondary crystallization takes place in newly formed smaller spherulites or within the already existing ones, can be decided by the values of the Avrami exponents. Interspherulitic crystallization is, of course, less hindered than interlamellar crystallization. The latter type of crystallization takes place within the spherulites of the primary crystallization and undergoes severe steric hindrances, because the newly built crystals have to grow in an already formed environment. Consequently, the Avrami exponents should be very low. Owing to the fact that the nucleation of these crystals is secondary, and that no three-dimensional undisturbed growth can be expected, the values for n should be around 1. Fig. 2b shows a plot of these values for both blend systems. Indeed, n is below 1 and varies around 0.8. For the blend containing TOR, n drops from 0.8 for neat polypropylene to $n = 0.7$ and increases to $n = 1.1$ for the sample containing 20% TOR. The values roughly correlate with the course of the interlamellar distances of the iPP/TOR lamellar morphology as a function of TOR concentration [2]: this distance, calculated from interface distribution functions, decreases for TOR concentrations around 10%. For the iPP/EPDM blend, an interlamellar distance is observed, which increases slightly for low EPDM concentrations, and decreases for concentrations $> 10\%$ [28]. The Avrami exponent follows roughly this course, except for the value at 20% EPDM. In principle, the dependence of the Avrami-exponent on the elastomer concentration seems to be an effect of the interlamellar volume. We further find that the elastomer affects both the primary and secondary crystallization.

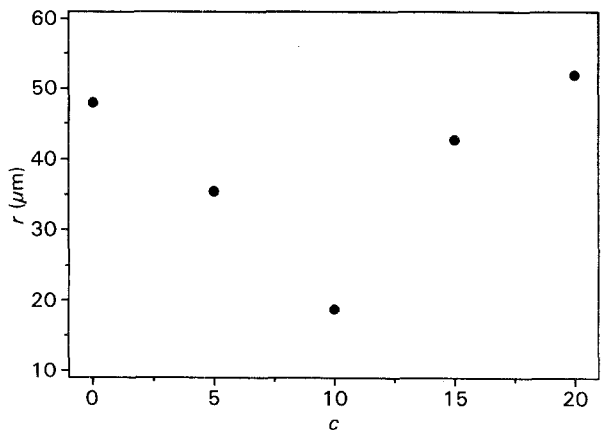

Figure 4 Mean spherulitic radius as a function of elastomer concentration.

From these results we draw the following conclusions.

1. The elastomers trans-polyoctenylene and ethylene–propylene–diene–terpolymer have, when mixed to isotactic polypropylene, different effects on the crystallization behaviour of the iPP.
2. Both primary and secondary crystallization can be well determined by measuring the X-ray crystallinity as a function of crystallization time.
3. Avrami exponents, determined by X-ray scattering, match well with values measured by optical microscopy.
4. Secondary crystallization takes place within the already formed spherulites and increases the crystallinity of the sample.
5. The size distribution of the spherulitic microstructure is not changed by the secondary crystallization.
6. For iPP/TOR blends, the spherulitic radius depends on the composition; in iPP/EPDM blends the elastomer does not influence the radius of the spherulites.

References

1. R. KOSFELD, K. SCHAEFER, E. A. HEMMER and M. HESS, in "Integration of Fundamental Polymer Science and Technology", edited by L. A. Kleintjens and P. J. Lemstra, Rolduc Polymer Meeting 4 (Elsevier, London, New York, 1989).
2. W. WENIG and H.-W. FIEDEL, *Makromol. Chem.* **192** (1991) 85.
3. E. MARTUSCELLI, C. SILVESTRE and L. BIANCHI, *Polymer* **24** (1983) 1458.
4. W. WENIG and H.-W. FIEDEL, *Makromol. Chem.* **192** (1991) 191.
5. H. E. KISSINGER, *Anal. Chem.* **29** (1957) 1702.
6. K. MATUSITA and S. SAKKA, *J. Non-Cryst. Solids* **38/39** (1980) 741.

7. D. W. HENDERSEN, *ibid.* **30** (1979) 301.
8. P. G. BOSWELL, *J. Mater. Sci.* **15** (1980) 1939.
9. J. N. HAY, *Br. Polym. J.* **11** (1979) 137.
10. K. HARNISCH and H. MUSCHIK, *Colloid Polym. Sci.* **261** (1983) 908.
11. L. S. REMALY and J. M. SCHULTZ, *J. Appl. Polym. Sci.* **14** (1970) 1871.
12. A. WASIAK, *Chemtracts-Macromol. Chem.* **2** (1991) 211.
13. A. WEIDINGER and P. H. HERMANS, *Makromol. Chem.* **50** (1961) 98.
14. G. BODOR, M. GRELL and A. KALLO, *Faserforsch. Textiltechn.* **15** (1964) 527.
15. F. RYBNIKAR, *Kunststoffe* **57** (1967) 199.
16. C. G. VONK, *J. Appl. Crystallogr.* **6** (1973) 158.
17. M. AVRAMI, *J. Chem. Phys.* **7** (1939) 1103.
18. *Idem, ibid.* **8** (1940) 212.
19. *Idem, ibid.* **9** (1941) 177.
20. L. MANDELKERN, "Crystallization of Polymers" (McGraw-Hill, New York, 1963).
21. F. L. BINSBERGEN, *J. Polym. Sci. Polym. Symp.* **59** (1977) 11.
22. J. P. MERCIER, *Polym. Eng. Sci.* **30** (1990) 270.
23. N. BILLON, J. M. ESCLEINE and J. M. HAUDIN, *Colloid Polym. Sci.* **267** (1989) 527.
24. H. W. STARKWEATHER and R. E. BROOKS, *J. Appl. Polym. Sci.* **1** (1959) 236.
25. T. I. SOGOLOVA, *Polym. Mech.* **1** (1965) 1.
26. Y. L. VINOGRADSKAYA, G. A. MOLCHANOVA and B. Y. TARASOV, *ibid.* **1** (1965) 5.
27. D. M. GEZOVICH and P. H. GEIL, *Polym. Eng. Sci.* **8** (1968) 210.
28. M. BROSE, Thesis, University of Duisburg (1991).

Received 14 September 1993
and accepted 21 March 1994